

NUCLEAR DATA AND MEASUREMENTS SERIES

ANL/NDM-15

Radiative Capture of Fast Neutrons in ^{165}Ho and ^{181}Ta

by

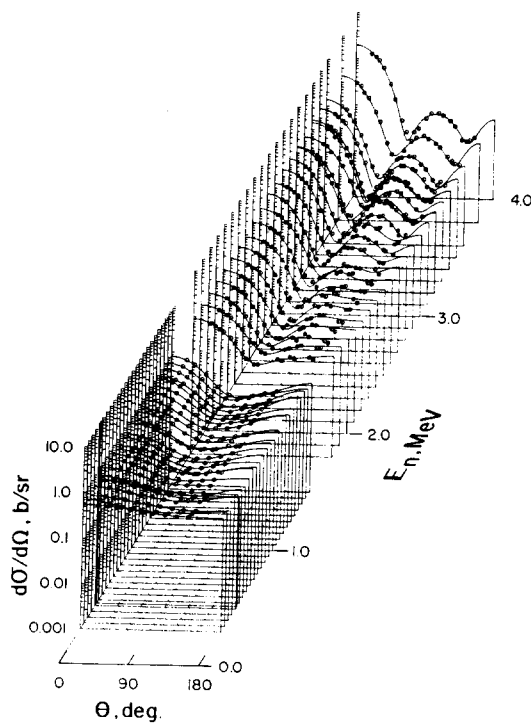
W.P. Poenitz

June 1975

**ARGONNE NATIONAL LABORATORY,
ARGONNE, ILLINOIS 60439, U.S.A.**

NUCLEAR DATA AND MEASUREMENTS SERIES

ANL/NDM-15
Radiative Capture of Fast Neutrons
in ^{165}Ho and ^{181}Ta
by
W. P. Poenitz
June 1975



UofC-AUA-USAEC

ARGONNE NATIONAL LABORATORY,
ARGONNE, ILLINOIS 60439, U.S.A.

The facilities of Argonne National Laboratory are owned by the United States Government. Under the terms of a contract (W-31-109-Eng-38) between the U. S. Atomic Energy Commission, Argonne Universities Association and The University of Chicago, the University employs the staff and operates the Laboratory in accordance with policies and programs formulated, approved and reviewed by the Association.

MEMBERS OF ARGONNE UNIVERSITIES ASSOCIATION

The University of Arizona
Carnegie-Mellon University
Case Western Reserve University
The University of Chicago
University of Cincinnati
Illinois Institute of Technology
University of Illinois
Indiana University
Iowa State University
The University of Iowa

Kansas State University
The University of Kansas
Loyola University
Marquette University
Michigan State University
The University of Michigan
University of Minnesota
University of Missouri
Northwestern University
University of Notre Dame

The Ohio State University
Ohio University
The Pennsylvania State University
Purdue University
Saint Louis University
Southern Illinois University
The University of Texas at Austin
Washington University
Wayne State University
The University of Wisconsin

NOTICE

This report was prepared as an account of work sponsored by the United States Government. Neither the United States nor the United States Atomic Energy Commission, nor any of their employees, nor any of their contractors, subcontractors, or their employees, makes any warranty, express or implied, or assumes any legal liability or responsibility for the accuracy, completeness or usefulness of any information, apparatus, product or process disclosed, or represents that its use would not infringe privately-owned rights.

ANL/NDM-15
Radiative Capture of Fast Neutrons
in ^{165}Ho and ^{181}Ta

by

W. P. Poenitz

June 1975

In January 1975, the research and development functions of the former U.S. Atomic Energy Commission were incorporated into those of the U.S. Energy Research and Development Administration.

Applied Physics Division
Argonne National Laboratory
9700 South Cass Avenue
Argonne, Illinois 60439
U.S.A.

NUCLEAR DATA AND MEASUREMENTS SERIES

The Nuclear Data and Measurements Series presents results of studies in the field of microscopic nuclear data. The primary objective is the dissemination of information in the comprehensive form required for nuclear technology applications. This Series is devoted to: a) Measured microscopic nuclear parameters, b) Experimental techniques and facilities employed in data measurements, c) The analysis, correlation and interpretation of nuclear data, and d) The evaluation of nuclear data. Contributions to this Series are reviewed to assure technical competence and, unless otherwise stated, the contents can be formally referenced. This Series does not supplant formal journal publication but it does provide the more extensive information required for technological applications (e.g., tabulated numerical data) in a timely manner.

TABLE OF CONTENTS

	<u>Page</u>
ABSTRACT.	3
I. INTRODUCTION.	4
II. EXPERIMENTAL TECHNIQUES	5
III. EXPERIMENTAL RESULTS.	6
1. Measurements and Normalization	6
2. Corrections.	7
3. Results and Uncertainties.	8
IV. MODEL CALCULATIONS.	10
1. Radiative Capture and Activation Cross Sections.	11
2. Neutron Transmission Coefficients.	12
3. Nuclear Level Density.	13
4. Gamma Transition Probabilities	13
5. Gamma Cascade Statistics	13
6. Results and Discussion of the Model Calculations	14

Radiative Capture of Fast Neutrons
in ^{165}Ho and ^{181}Ta *

by

W. P. Poenitz

ABSTRACT

The fast neutron capture cross sections of ^{165}Ho and ^{181}Ta were measured from 0.3 to 3.0 MeV. A 1300g large liquid scintillator with a time-resolution of 3 - 4 nsec was used for the detection of capture events. The time-of-flight technique was utilized for background suppression. A Grey Neutron Detector was used as a neutron flux monitor. The data were normalized at 500 keV to the standard capture cross section of gold. The resulting cross sections had an uncertainty of about 7 percent.

The present capture cross sections and activation cross sections reported in the literature were interpreted in terms of the statistical model, using the Hauser-Feshbach formalism and the gamma-cascade model (1).

* This work performed under the auspices of the U.S. Energy Research and Development Administration.

I. INTRODUCTION

Fast neutron capture and activation cross sections are of considerable interest to fission and fusion reactor evaluators in connection with neutron absorption losses, gamma-ray production and after-heat problems; to nuclear theory; and to cosmological theories of element formation. These important applications have led to a large number of measurements applying a variety of experimental techniques. The detection of fast neutron capture rates falls into two main categories:

- 1) The detection of prompt gamma-rays with a large liquid scintillator (Diven et al. (2), Gibbons et al. (3)), by a proportional counter (Konks et al. (4)), or a Moxon-Rae detector (Moxon and Rae (5), Macklin et al. (6)), and
- 2) The detection of the induced radioactivity (for example, Johnsrud et al. (7)). A large liquid scintillator which was used in the present experiments has the advantage of more general applicability to the capture-event detection than the activation technique, and, compared to other techniques of the first group allows the discrimination against $(n, n'\gamma)$ and $(n, \gamma n')$ events.

The determination of the absolute neutron flux is most commonly avoided in capture cross section measurements by using a standard cross section as a reference. The capture cross section of gold, which has been established as a standard capture cross section (8,9), was used in the present experiments.

Few data are available for the fast neutron capture cross section of ^{165}Ho . A discrepancy exists around 400 keV between recent data by Czirr and Stelts (10) and older data by Johnsrud et al. (7). Experimental values for the capture cross section of ^{181}Ta are more abundant but scatter over a 30 percent range in magnitude, at some energies even over a 100 percent range. Thus, the

measurements of additional data on both nuclei are desirable.

The neutron capture in both, ^{165}Ho and ^{181}Ta , results in nuclei with isomeric states. This allows the investigation of the statistical behavior of gamma-cascades which de-excite the compound states. Model calculations of the capture and activation cross sections were carried out in terms of the statistical model. The Hauser-Feshbach formalism and a previously described gamma-cascade model (1) were used in the calculations. A systematic investigation of the accuracy with which such models can predict these cross sections is of practical interest. Many capture cross sections or activation cross sections of fission product nuclei or neutron capture products of materials involved in fission reactor construction are difficult to measure. Calculated cross sections are often the only means of predicting their influence on reactor neutronics and after heat problems.

II. EXPERIMENTAL TECHNIQUES

Measurements were carried out using "monoenergetic" neutrons produced with the $^7\text{Li}(p,n)^7\text{Be}$ reaction. Metallic lithium targets with thicknesses resulting in incident neutron resolutions between 32 and 54 keV were used. A pulsed and bunched proton beam was accelerated by the Argonne Tandem-Dynamitron. The repetition rate was 2 MHz and the pulse width was 1 - 2 nsec. The capture gamma-ray detector was a 1300-liter iron tank filled with a liquid scintillator. The scintillation light was viewed by twelve AVP57 multipliers. The time-resolution of the detector was 3 - 4 nsec and the gamma energy resolution was 26 percent for ^{60}Co (FWHM). A threshold corresponding to a 2 - 3 MeV gamma ray energy was set in order to eliminate the detection of $(n,n'\gamma)$ and $(n,\gamma n')$ events.

The samples consisted of metallic holmium, tantalum or gold discs with a diameter of 8.0 cm and thicknesses of 0.13, 0.10 and 0.08 cm, respectively. They were positioned in a flight path 2.5 m from the neutron source in the center of a channel through the large liquid scintillator tank. The Grey Neutron Detector was used as a flux monitor. Because of the normalization to the capture cross section of gold at 500 keV only the energy dependence of this detector was utilized. A detailed description of this detector and its efficiency was given elsewhere (11).

The time-of-flight technique was used for background suppression with the capture gamma-ray detector. Measurements with lead and carbon samples were used to determine background events caused by neutrons scattered in the sample and captured in structural material of the detector. This background was found to be small (< 1%) for the cross sections measured in the present experiment. The background of the neutron detector was determined with a closed collimator channel. A more detailed description of the experimental techniques was previously given (12,13).

III. EXPERIMENTAL RESULTS

1. Measurements and Normalization

Measurements of the cross section shapes of ^{165}Ho and ^{181}Ta were carried out in the 0.3 to 3.0 MeV energy range. The ratios of the capture cross sections of ^{165}Ho and ^{181}Ta to ^{197}Au were measured at 0.5 MeV. An on-line computer system (14) was used for the data acquisition. The time-of-flight spectrum of the capture γ -ray detector, the energy spectrum coincident with the neutron capture peak in the time-of-flight spectrum, the energy spectrum coincident with

an equally spaced interval in the time-of-flight spectrum adjacent to the neutron peak, and the neutron monitor spectrum were recorded. Measurements of the energy dependence of the capture cross sections of holmium and tantalum were repeated 2 - 3 times, the ratio relative to the capture cross section of gold at 500 keV was repeated 4 - 5 times. Agreement was found within the statistical uncertainties and the average values were used. A value of 138 mb for the capture cross section of gold at 500 keV was used for the normalization of the data. This value was obtained in an evaluation of a consistent set of standard cross sections (15).

2. Corrections

Neutrons scattered elastically once or more times within the sample have an increased probability for capture due to the larger average flight path after the collision. Furthermore, neutrons scattered inelastically have an increased capture probability due to their energy loss. The neutron scattering in the sample causes a flux attenuation of the primary beam which affects both the primary capture rate and the neutron detection. Corrections for these effects were calculated with the Monte Carlo technique. The angular distribution of the elastic scattering, the energy loss in the inelastic scattering process, and the energy dependence of the various cross sections were taken into account. Neutrons were followed up to three collisions in the sample. The corrections for ^{165}Ho and ^{181}Ta were in the 7 - 13 percent range and did not vary as strongly with energy as, for example, the correction for ^{93}Nb (13). The reason is the relatively steady decrease of the capture cross sections of ^{165}Ho and ^{181}Ta with increasing energy and the relatively uniform dis-

tribution of levels contributing to inelastic scattering.

The efficiency for the detection of a γ -capture event is given by two factors: 1) the probability of a γ -interaction in the detector, and 2) the probability that the resulting energy signal is above the threshold set for the elimination of $(n,n'\gamma)$ and $(n,\gamma n')$ events. The three nuclei, ^{165}Ho , ^{181}Ta and ^{197}Au have similar neutron binding energies, 6.2, 6.1 and 6.5 MeV respectively. Thus, the extrapolation to zero pulse height was carried out with an empirical formula for the shape of the energy spectrum. A correction of 2 percent was applied for the leakage of high energy gamma-rays from the tank. Such high energy transitions are more frequent in ^{198}Au than in ^{166}Ho and ^{182}Ta , and the correction for ^{198}Au was 3 percent.

Other corrections were made for the transmission of the neutron beam through the air between the sample and the neutron monitor, the energy dependence of the neutron flux monitor, and for neutrons with energies other than the primary neutron group coming from the source. These corrections were previously discussed in detail (12,13).

3. Results and Uncertainties

The present results are given in Table I and shown in Figs. 1 and 2. The energy uncertainty of less than 3 keV is negligible in the context of the present measurements. The second column in Table I gives the energy resolution which was determined from the target thickness and the stopping cross section of the target material. Sources of uncertainties are listed in Table II. Under "statistics" the statistical uncertainty (one standard deviation) or the reproducibility (difference between the several sets of data) is given--whichever was the larger. The uncertainties and the resolution of the measurements is indicated in the figures by the size of the symbols. The present data for

^{165}Ho were compared in Fig. 1 with data by Czirr and Stelts (10) and Johnsrud et al. (7). The original data by Johnsrud et al. were activation cross sections for the isomeric state of ^{166}Ho . They were corrected for newer fission cross section values (12, 16) and for the capture resulting in ^{166}Ho in its ground states by

$$\sigma_{n,\gamma}(^{165}\text{Ho}) = \sigma_{\text{act}}(^{166}\text{Ho}^{\text{m}}) \cdot \left(1 + \frac{\sigma_{\text{act}}(^{166}\text{Ho}^{\text{g}})}{\sigma_{\text{act}}(^{166}\text{Ho}^{\text{m}})} \right)$$

where $\sigma_{\text{act}}(^{166}\text{Ho}^{\text{g}})/\sigma_{\text{act}}(^{166}\text{Ho}^{\text{m}})$ was obtained by theoretical calculations as outlined in Section IV of this paper. This correction term is 15-30%. The agreement with the data by Johnsrud et al. (7) is reasonable. A difference of about 30 percent exists between the present data and those by Czirr and Stelts at 400 keV. A similar difference appears to exist for the capture cross section of gold which Czirr and Stelts measured together with ^{165}Ho . An eyeguide curve was drawn through the present data for Ta as shown in Fig. 2 and compared in Figs. 3a and b with other data. Not shown are data by Miskel et al. (17) which scatter over a range exceeding a factor of 2. Data by Diven et al. (2) and by Friesenhahn (18) are systematically higher than the present results. The agreement is good with data by Hellstroem et al. (19), Cox (20), Brzosko et al. (21) and Lindner et al. (22). However, the data by Lindner et al. do not show quite as pronounced a "bump" in the cross section between 1 and 2 MeV as the present data and those by Cox (20) and by Hellstroem et al. (19). A point at 2.9 MeV by Lindner et al. is lower than the present results and values by Brzosko et al. above 3 MeV appear to be higher.

IV. MODEL CALCULATIONS

The present theoretical calculations of fast neutron capture cross sections in the lower MeV energy range are based on the statistical model. The basic formalism was developed more than two decades ago (23, 24, 25) and was applied in many systematic calculations of fast neutron capture cross sections (26, 27, 28). The agreement between theoretical results and experimental values was not always satisfactory. Discrepancies of a factor of 2 were found (29) which could not be explained by the uncertainty of the experimental values. Other theoretical calculations resulted in a relatively good description of experimental values (28, 30, 31). However, different model calculations resulted in values differing by more than a factor of 2 (28). Whereas there are many publications dealing with the calculation of activation cross sections at thermal neutron energy, only a few concern the calculation of fast neutron activation cross sections (13, 34-34, 36). In many cases the (n, γ) process leads to identical capture and activation cross sections. However, in some nuclei, isomeric states exist and several activation cross sections can be determined. The calculation of such activation cross sections follows the same procedure as used in the calculation of capture cross sections. However, the probability for the γ -cascade which de-excites the compound nucleus ending in the isomeric state or the ground state must be included. Vandenbosh and Huizenga (35) described a model for the calculation of such probabilities. This model was used by Grench et al. (33) to calculate isomeric ratios for fast neutron capture. A more realistic model for the description of γ -ray cascades de-exciting a compound nucleus was described previously (1), and applied in the calculation

of fast neutron activation cross section of ^{103}Rh , ^{109}Ag and ^{115}In (36) and of ^{93}Nb and ^{94}Nb (13).

The calculation of neutron activation and capture cross sections requires the knowledge of neutron transmission coefficients, γ -transition probabilities and nuclear level densities. Most changes in more recent theoretical calculations concern improved models for the gamma-ray transition probabilities (37-40). In view of the difficulty in measuring most of the important capture cross sections of fission product nuclei as well as some activation cross sections, further study of fast neutron capture and activation cross sections appears desirable.

1. Radiative Capture and Activation Cross Sections

For the present calculations, the target and the compound nuclei are assumed to have discrete levels with known energies, spins and parities, (E_i, I_i, π_i) , and level continuum ranges described by a level density formula, $\rho(E, I, \pi)$. Fig. 4 shows the schematic level schemes for ^{181}Ta and ^{182}Ta . A proper application of the Hauser-Feshbach formalism to these level schemes results in an expression for the cross section for the occupation of the low lying level i of the compound nucleus:

$$\sigma(n, \gamma \rightarrow i) = \frac{1}{2(2I+1)} \frac{\pi}{k^2} \sum_{\ell=0}^{\infty} \sum_{j=|\ell-\frac{1}{2}|}^{\ell+\frac{1}{2}} T_n(\ell, j, E) \cdot$$

$$\sum_{J=|j-I|}^{j+I} \frac{(2J+1) \cdot T_c(J, E) \cdot R \cdot B_i(J, E)}{\Gamma_\gamma(J, E) + \sum_m T_n(\ell', j'; E, E_m) + T_n^{\text{Con}}},$$

where I is the spin of the target nucleus ground state, k is the wave number, the T_n are the neutron transmission coefficients with T_n^{Con} accounting for inelastic neutron transitions to the continuum range of the target nucleus. T_c and T_γ are the capture and γ -radiation transmission

coefficients. B_1 is the probability for the γ -ray cascade which follows the decay of the compound nucleus to end on the low lying level i . R is a correction for replacing the average of a ratio with the ratio of the averages (41).

2. Neutron Transmission Coefficients

The capture cross section below the first inelastic level of the target nucleus does not depend strongly on the neutron transmission coefficients which occur in both, the numerator and the denominator of the Hauser-Feshbach formula and the neutron channel is the dominant exit channel at higher energies. The first few inelastic neutron channels may strongly influence the capture cross section (42) but at still higher neutron energies with many neutron exit channels contributing to the decay of the compound nucleus the influence of a single neutron channel is once again only slight. Of importance then is only a proper accounting for the effects of the contributing discrete levels. For the present calculations the neutron transmission coefficients for transitions to the discrete levels of the target nucleus were calculated with the optical model. The optical model code ABACUS (43) was used for the calculation. The parameters were those reported to fit well the elastic and inelastic scattering on ^{165}Ho and ^{181}Ta (44,45). Neutron transmission to the continuum range was calculated with the strong interaction model (see for example Ref. 46) and integrated with a level density given by the level density formula of the Fermi-gas model. The ^{181}Ta nucleus is strongly deformed. However, only spherical model calculations were carried out for the neutron transmission coefficients. It was shown by Fricke et al. (29) that the spherical model calculations and the deformed model calculations result in only minor differences for the capture cross sec-

tion (of ^{181}Ta).

3. Nuclear Level Density

The well known level density formula based upon the Fermi-gas model and modified for shell and pairing energy was used. The expressions and parameters used were summarized previously (13).

4. Gamma Transition Probabilities

Gamma transition probabilities were needed in the calculation of the gamma and capture widths and the low-lying-level occupation probabilities. The simplest model used in many calculations of gamma and capture widths is the single particle model by Weisskopf (23). A more realistic model for the decay of the compound nucleus by gamma ray emission was given by Axel (38). The transition probability is derived as the inverse process of the photo-nuclear absorption and shows the typical giant resonance character of this process. The implication of the different models and comparison with partial transition probabilities were discussed recently by Bollinger (37). The explanation of gamma ray spectra obtained with fast neutron capture required the introduction of an additional "pigmy" resonance (47). For the present calculations the Weisskopf, Axel and Pigmy resonance transition probabilities were optional alternatives. In addition to dipole transitions also quadrupole transitions were allowed. A distinction was made between the total gamma radiation width and the total capture width using in the calculations as an approximation the assumption that all gamma transitions to levels above the neutron binding energy result in $(n,\gamma n')$ processes.

5. Gamma Cascade Statistics

A model previously described (1) was used in the present calculation of low lying level occupation probabilities. However, the optional choice of Weisskopf, Axel and Pigmy resonance transitions was also applied to these calculations.

In the case of ^{165}Ho , previous measurements of low lying level occupation probabilities in resonances in the eV-range were available (48) and resulted in a good agreement between the theoretical calculations and the experimental values.

An additional check for the theoretical model can be made with the thermal isomeric cross section ratio. Using the cross sections from a recent compilation (49) one obtains 0.056 and 0.00049 for the isomeric cross section relative to the ground state cross section for ^{165}Ho and ^{181}Ta , respectively. The values calculated with the present model are 0.062 and 0.122 for Holmium and 0.0001 and 0.0005 for Tantalum for the spin 3 and spin 4 compound state values, respectively. In the case of ^{181}Ta , the contribution from the first (4.28 eV) resonance which has a spin of 4 to that of the second resonance which has a spin of 3 is about 9:1. Thus, the theoretical value of 0.0005 should be compared with the experimental value of 0.00049; an excellent and probably fortunate agreement.

6. Results and Discussion of the Model Calculations

Tantalum was considered an interesting indicator for the validity of the models used in the calculation of the activation cross sections because of the high spin value (10^-) of its isomeric state. The fast neutron activation cross section for this state (16 min half life) is about two orders of magnitude smaller than the neutron capture cross section. Experimental values were reported up to 1.6 MeV by Cox (20).

Brzosko et al. (40) calculated γ -ray spectra and fast neutron capture cross sections for a number of elements including ^{181}Ta using the Axel γ -ray transition probabilities. They suggested that Ta requires a Pigmy resonance contribution as well as all the other elements for which they carried out model calculations.

though the γ -ray spectrum does not show the anomalous bump in the 5 - 6 MeV range. This difference from a previous conclusion by Starfeld et al. (47) was explained with a larger spin-cut-off factor required for the strongly deformed tantalum nucleus. A more recent calculation by Gardner (50) uses assumptions very similar to those used by Brzosko et al. (40). However, two giant dipole resonances were assumed as appropriate for a deformed nucleus, the Pigmy resonance contribution was one order of magnitude less, and a cutoff was assumed for the γ -strength-function. Weisskopf transition probabilities were also used by both, Brzosko et al. (40) and Gardner (50). The calculations by Brzosko et al. show an appreciable difference between the calculated cross sections for the two different transition probabilities above 400 keV, whereas the results by Gardner (50) indicate a much smaller difference, especially below 1 MeV.

In the present calculations, the sensitivity to many of the parameters and model assumptions was investigated. Results are shown in Fig. 5 and compared with the present experimental values. The solid curves were obtained with Axel and 1 percent Pigmy resonance transition probabilities. Only one giant resonance was used in the calculation of these curves because separate calculations showed that there is only a negligible difference between the cross sections obtained with one (spherical model) or two (deformed model) giant resonances. The dotted curve was obtained without a Pigmy resonance contribution. The difference is small and less than the uncertainty of the experimental values. A similarly small difference was obtained for the isomeric cross section, thus the fast neutron cross sections are not helpful in determining the existence or the amount of contributions from a Pigmy resonance.

The dashed curves in Fig. 5 were obtained by using the Weisskopf transition probabilities. It is obvious that the use of the Axel γ -transition probabilities results in improved cross section predictions. The difference between the two obtained in the present calculations supports more likely the calculations by Gardner (50) rather than those by Brzosko et al. (40).

All curves labeled A in Fig. 5 were obtained with the use of parameters in the level density formula which apply over a wide mass range of nuclei. Curves labeled C indicate the effect caused by an increase in the spin-cut-off factor σ which is suggested for a deformed nucleus like ^{181}Ta (51). Though the results for the total capture cross section improves the comparison with experimental values, the activation cross section clearly suggests that such increase of the spin-cut-off factor is undesirable.

Fig. 6 shows the result of the model calculation for the neutron capture and activation cross sections of ^{165}Ho . There are no experimental values available for the activation cross section of the long living isomeric state. The calculations were carried out for Axel γ -transition probabilities and a 1 percent Pigmy resonance contribution. The agreement with the present (n,γ) cross sections and with the activation cross sections for the 27.2 h half life as measured by Johnsrud et al. (7) is good.

REFERENCES

1. W. P. Poenitz, *Z. f Physik* 197, 262 (1966).
2. B. C. Diven, J. Terrell and A. Hemmendinger, *Phys. Rev.* 120, 556 (1960).
3. J. H. Gibbons, R. L. Macklin, P. D. Miller and J. H. Neiler, *Phys. Rev.* 122, 182 (1961).
4. V. A. Konks, Y. P. Popov, F. L. Shapiro, *Soviet Phys. (JETP)* 19, 59 (1964).
5. M. C. Moxon, E. R. Rae, *Nucl. Instr.* 24, 445 (1963).
6. R. L. Macklin et al., *Nucl. Phys.* 43, 353 (1963).
7. A. E. Johnsrud, M. G. Silbert, H. H. Barschall, *Phys. Rev.* 116, 927 (1959).
8. Panel on "Nuclear Standards Needed for Neutron Cross Section Measurements", Brussels 1967, IAEA-107.
9. Second Panel on "Neutron Standard Reference Data", IAEA, Vienna 1972.
10. J. B. Czirr and M. L. Stelts, *Nucl. Sci. & Eng.* 52, 299 (1973).
11. W. P. Poenitz and E. Wattecamps, EANDC-33 "U", 102 (1963),
W. P. Poenitz, *Nucl. Instr. and Methods* 58, 39 (1968),
W. P. Poenitz, *Nucl. Instr. and Methods* 72, 120 (1969),
W. P. Poenitz, Proc. of Second Panel on Neutron Standard Reference Data, p. 47, IAEA, Vienna (1972).
12. W. P. Poenitz, *Nucl. Sci. Engineering*, 53, 370 (1974).
13. W. P. Poenitz, Argonne National Laboratory, ANL/NDM-8 (1974).
14. W. P. Poenitz and J. F. Whalen, Argonne National Laboratory, ANL-8026 (1973).
15. W. P. Poenitz, Symp. on Neutron Standards and Flux Normalization, AEC Symposium Series 23, CONF-701002 p. 331, Argonne (1970).
16. I. Szabo, J. L. Leroy, and J. P. Marquette, Conf. on Neutron Physics, Kiev 1973 (Vol. II p. 27).
17. J. A. Miskel, K. V. Marsh, M. Lindner, R. J. Nagle, *Phys. Rev.* 128, 2717 (1962).
18. S. J. Friesenhahn, W. M. Laper, M. P. Fricke, D. G. Costello, and A. D. Carlson, Gulf General Atomic, GA-10194, (1970).
19. L. Hellstroem et al., *J. Nucl. Eng.* 27, 71 (1973).
20. S. A. Cox, *Phys. Rev.* 133B, 378 (1964).

21. J. S. Brzosko, E. Gierlik, A. Soltan, Jr., and Z. Wilhelmi, Nucl. Phys. A123, 603 (1969).
22. M. Lindner, R. J. Nagle and J. H. Landrum, Lawrence Livermore Laboratory, UCLR-75838 (1974).
23. J. M. Blatt, V. F. Weisskopf, Theoretical Nuclear Physics, John Wiley & Sons, N. Y. (1952).
24. W. Hauser and H. Feshbach, Phys. Rev. 87, 366 (1952).
25. B. Margolis, Phys. Rev. 88, 327 (1952).
26. V. Benzi and M. V. Bartolani, IAEA-Conf. on Nucl. Data for Reactors, Vol. I, CN-23/115, Vienna (1967).
27. J. L. Cook, Conf. on Nucl. Data for Reactors, Vol. I, 549. IAEA (1967).
28. F. Schmittroth, Hanford Eng. Dev. Lab., ENDF-195.
29. M. P. Fricke et al., Conf. on Nucl. Data for Reactors, Vol. II, 281, IAEA (1970).
30. V. Benzi and M. V. Bartolani, Conf. on Nucl. Data for Reactors, Vol. I, 537, IAEA (1970).
31. V. Benzi et al., Comitato Nazionale Energia Nucleare, RT/I(69)44 (1969).
32. J. Csikai et al., Nucl. Phys. 41, 316 (1963).
33. H. A. Grench et al., Nucl. Phys. A94, 157 (1966).
34. W. P. Poenitz, Conf. on Nucl. Cross Sections and Technology, Washington (1975).
35. I. R. Huizenga, and R. Vandenbosch: Phys. Rev. 120, 1305 (1960).
36. W. P. Poenitz, Phys. Kerhandlungen, 17J., 21 (1966), W. P. Poenitz, Thesis, Technical Univ. Karlsruhe (1966).
37. L. M. Bollinger, Conf. on Nuclear Structure, p. 317, IAEA, Vienna (1968).
38. P. Axel, Phys. Rev. 126, 671 (1962).
39. A. G. Dovbenko, A. V. Ignatyuk, and V. A. Tolstikov, International Nuclear Data Committee, INDC(CCP)-431L, p. 201 (1974).
40. J. S. Brzosko, E. Gierlik, A. Soltan Jr., and Z. Wilhelmi, Can. J. Physics 47, 2849 (1969).
41. A. M. Lane and J. E. Lynn, Proc. Phys. Soc. A70, 557 (1957).
42. C. Mossin-Kotin, B. Margolis and E. S. Troubetzkay, Phys. Rev. 116, 937 (1959).
43. E. H. Auerbach, Brookhaven National Laboratory, BNL-765 (1962).

44. A. B. Smith, P. T. Guenther, R. Hayes, and J. F. Whalen, Argonne National Laboratory, ANL 7363 (1967).
45. J. Meadows, A. Smith, J. Whalen and T. D. Beynan, Z. Physik 243, 171 (1971).
46. M. A. Preston, Physics of the Nucleus, Addison-Wesley Pub. Co. Inc., N. Y. (1962).
47. N. Starfelt, Nucl. Phys. 53, 397 (1964).
48. W. P. Poenitz and J. R. Tatarczuk, Nucl. Phys. A151, 569 (1970).
49. S. F. Mughabghab and D. I. Garber, Neutron Cross Sections, Vol. I, Resonance Parameters, Third Ed., BNL-325 (1973).
50. D. G. Gardner, Bull. Am. Phys. Soc., Vol. 19, No. 9, 1017(1974).
51. B. R. Mottelson and S. G. Nilsson, Kgl Danske Videnskab. Selskab Mat. Fys. Kr. 1, No. 8 (1959).
52. O. A. Wasson, R. E. Chrien, M. A. Love, M. R. Bhat, and M. Beer, Nucl. Phys. A132, 161 (1969).
53. R. G. Helmer, R. C. Greenwood, and C. W. Reich, International Symposium on Neutron Capture Gamma-Ray Spectroscopy, Studsvik (1969).
54. Nuclear Data Sheets for A=181 and A=182.
55. R. L. Macklin and J. H. Gibbons, Bull. Am. Phys. Soc. 11, 167 (1966).

TABLE 1. Results for the Fast Neutron Capture Cross Sections of ^{165}Ho and ^{181}Ta .

E_n/MeV	$\Delta E_n/\text{MeV}$	^{165}Ho		^{181}Ta	
		σ/mb	$\Delta\sigma/\text{mb}$	σ/mb	$\Delta\sigma/\text{mb}$
0.30	0.027			207	16
0.40	0.026	318	31	185	14
0.50	0.026	280	17	174	11
0.60	0.025	219	13	154	10
0.70	0.024	170	11	-	-
0.85	0.023	124	8	123	8
0.90	0.023	112	8	-	-
1.00	0.022	106	7	118	8
1.10	0.022	87.7	6.9	-	-
1.20	0.022	95.1	7.5	111	7
1.30	0.021	87.8	10.4	108	7
1.40	0.020	83.2	6.7	107	7
1.50	0.020	80.5	9.5	102	7
1.70	0.019	80.9	5.8	89.2	6.4
2.00	0.018	70.5	5.5	73.2	5.9
2.50	0.017	58.1	7.8	45.7	4.3
3.00	0.016	40.3	4.2	37.6	4.0

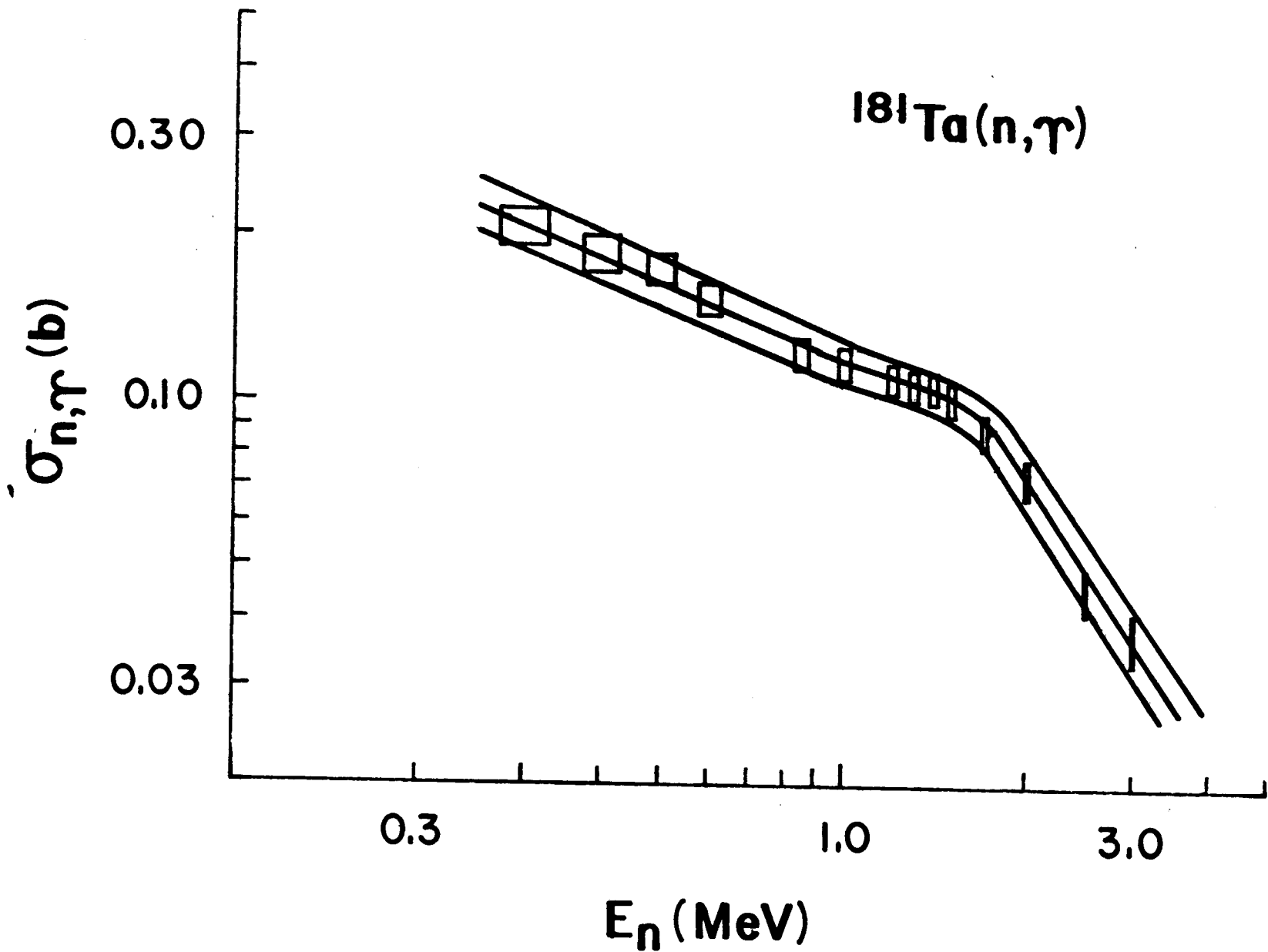
TABLE II. Uncertainties of the Capture Cross Section Measurements

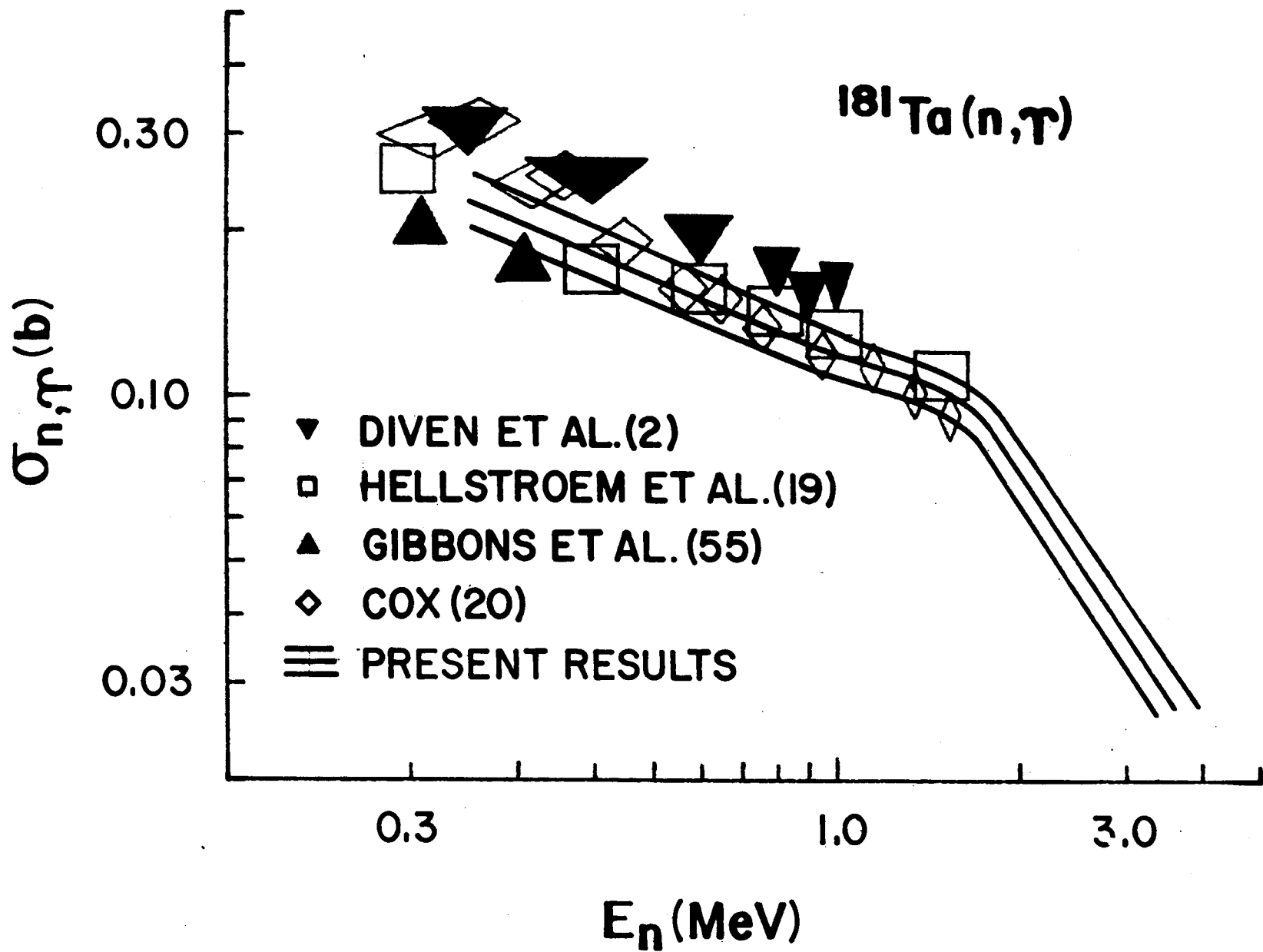
Source	Uncertainty Range/Percent
Statistics	1 - 5
Normalization	6.0
Neutron Monitor Efficiency*	0.0 - 2.6
Capture Detector Efficiency*	0.0 - 1.5
Correction for Scattered Neutrons*	0.0 - 3.0
Correction for Scattering in Air*	0.0 - 0.3
Sample Mass	0.5

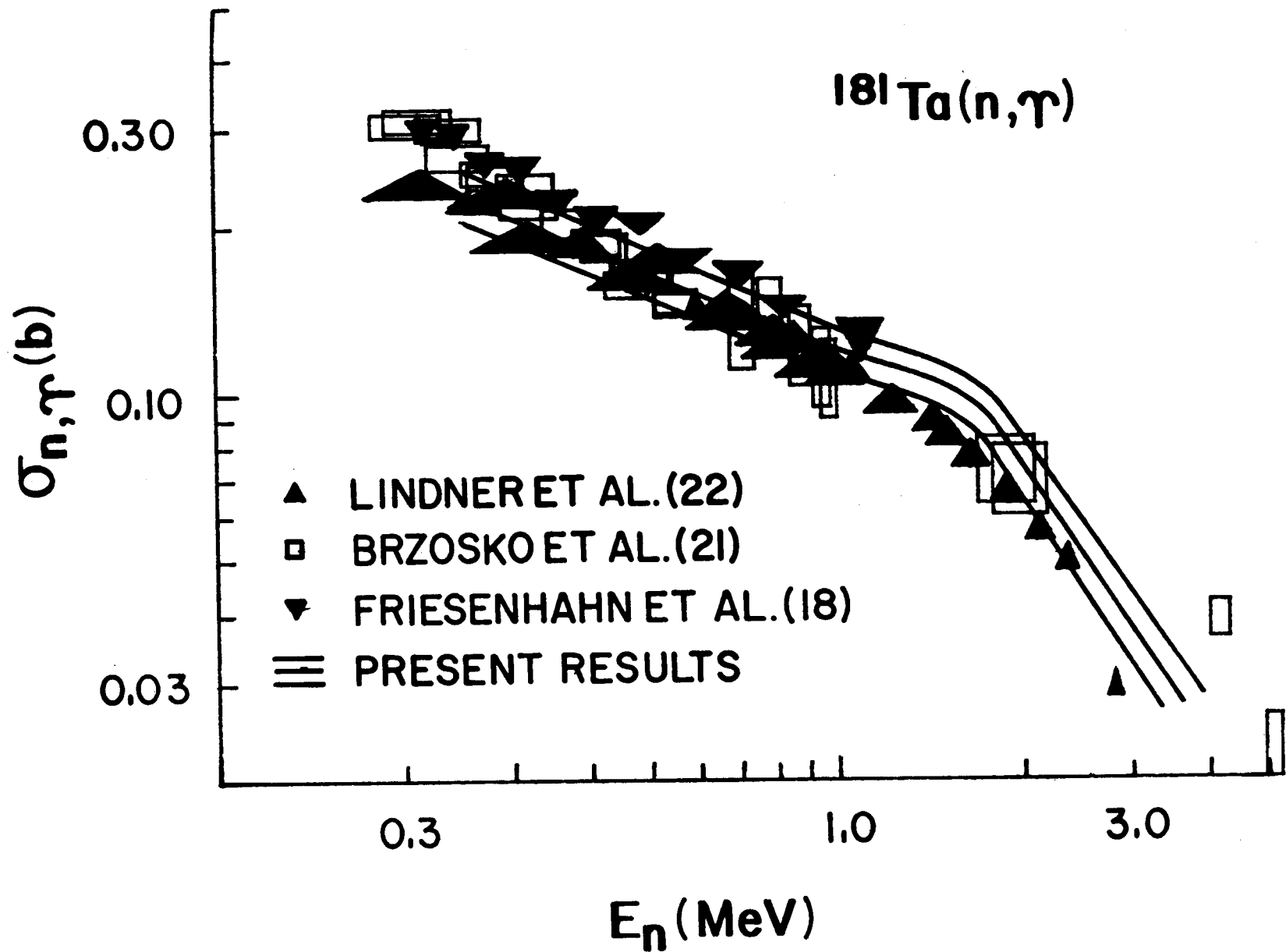
*The uncertainty of this correction is zero at the normalization point.

FIGURE CAPTIONS

- Fig. 1. Neutron Capture Cross Section of ^{165}Ho .
- Fig. 2. Neutron Capture Cross Section of ^{181}Ta - Present Results.
- Fig. 3a + b. Comparison of an Eye Guide Curve Through Present Results for ^{181}Ta with Other Data.
- Fig. 4. Level Schemes of ^{181}Ta and ^{182}Ta Used in the Present Model Calculations (see Ref. 52, 53 and 54).
- Fig. 5. Model Calculations for the Neutron Capture and Activation Cross Sections of ^{181}Ta (see text).
- Fig. 6. Model Calculations for the Neutron Capture and Activation Cross Sections of ^{165}Ho .







0.717 ————— 15/2+

0.619  3/2+
0.615  1/2+

0.548 ————— 15/2-

0.482 ————— 5/2+

0.519 ————— 10-

0.492 ————— 5+

0.479  4-

0.474  3+

0.402 ————— 2+

0.339 ————— 13/2-

0.360 ————— 3-

0.334  7+

0.331  5+

0.315 ————— 5-

0.301 ————— 11/2+

0.292 ————— 5-

0.270 ————— 2-

0.250 ————— 3+

0.237 ————— 5-

0.159 ————— 11/2-

0.173  5-

0.163 ————— 6+

0.136 ————— 9/2+

0.150  4+

0.114 ————— 4-

0.098 ————— 4-

0.006  9/2-
0.000  7/2+

0.016 ————— 5+

0.000  3-

181Ta

182Ta

